

Atmospheric CO₂: A finite reservoir model reproduces ¹⁴C / ¹³C over two centuries and indicates the fossil-fuel anthropogenic contribution.

Dr S E Taylor

Director, Geomatix Ltd, UK

set@geomatix.net

Keywords: CO₂ residence-time, CO₂ lifetime, carbon cycle, CO₂ atmospheric flux, anthropogenic emissions, global warming, climate change.

12 May 2022

Abstract

Whereas many carbon cycle models track CO₂ perturbations relative to a pre-industrial equilibrium, this paper uses absolute quantities to describe atmospheric CO₂ sinks, source and flow rates. This method, when combined with the notion of source and sink resistance, and a finite biospheric reservoir, accurately describes ¹⁴C levels between 1820 and 2020 using only five external parameters. The inputs are:- global records of fossil-fuel emissions, records of CO₂ mixing-ratio and listings of atmospheric atomic weapons tests. Over the same period ¹³C flows are also accurately described given a δ¹³C value for fossil fuel and a δ¹³C value for the initial background. This top-down approach differs from complex climate models since it circumvents the necessity to catalogue individual processes. The paper proceeds to use the method to examine the anthropogenic fossil-fuel emissions contributions during the period 1750 to 2020, deducing that around 24% remains in the atmosphere, while 76% has been absorbed in the land, terrestrial biosphere and surface ocean. During the same period 13% of the total CO₂ atmospheric concentration is due to fossil fuels. However, regarding the increase, fossil fuels contributed to 38% of the rise during this period.

1. Introduction.

The annual flux of carbon dioxide (CO₂) to the atmosphere forms a key part of the global carbon budget (Friedlingstein P. et al, 2020). In most climate models the carbon-cycle parameters are defined as being relative to a pre-industrial equilibrium where departures from equilibrium are considered as anthropogenic perturbations. The classic Bern model (Strassmann and Joos, 2018) is an example of this, where a series of carbon reservoirs representing land, ocean, atmosphere and deep ocean, initially holding equilibrium levels, are connected. Each reservoir has its own time-constant, while the connections between the reservoirs linearly relate the difference in carbon potential to flow. Yet it is clear this approach cannot be correct. Experience tells us that the rate of fire or respiration would not materially decrease if the CO₂ atmospheric level were marginally to increase, whereas on the other hand, plant growth responds to small increases in CO₂ level, as is evidenced by the increase in plant growth in greenhouses when supplied with artificial CO₂, or in the phenomenon of global greening (Zhu Z., et al., 2016). Hence, in practice we can see that although source flows are largely unaffected by changes in atmospheric CO₂ content, sink flows are significantly affected. The linear perturbation models with their simple flow

Atmospheric CO₂: A finite reservoir model reproduces 14C / 13C over two centuries and indicates the fossil-fuel anthropogenic contribution.

restriction between each reservoir do not make this distinction between source and sink resistance to flow, despite its obvious significance. In this paper sink flows, having the lower resistance, mainly determine the atmospheric lifetime while source flows, having a higher resistance and internal pressure, contribute to the ambient level without contributing significantly to the lifetime, because their resistance is too high. Lifetime relates capacity to drain rate; its importance being illustrated by the following question. "If all CO₂ emissions were extinguished (including respiration, fire etc) leaving gaseous absorption and photosynthesis to absorb CO₂, what would be the rate of fall of global atmospheric CO₂?" The Berne model cannot answer this question, because it has no absolute drain mechanism; it is an equilibrium model. However in this model, the sinks, whose flow rate is proportional to pressure, continuously drain away the CO₂ which is replenished by the sources if present. It represents a radically different approach, where sources and sinks have very different properties. This paper describes how the approach can be used to account for the variation of atmospheric 14CO₂ and 13CO₂ with time and to calculate the nett contribution of fossil fuel CO₂ emissions to modern day levels.

2. CO₂ Finite Reservoir (CFR) Model

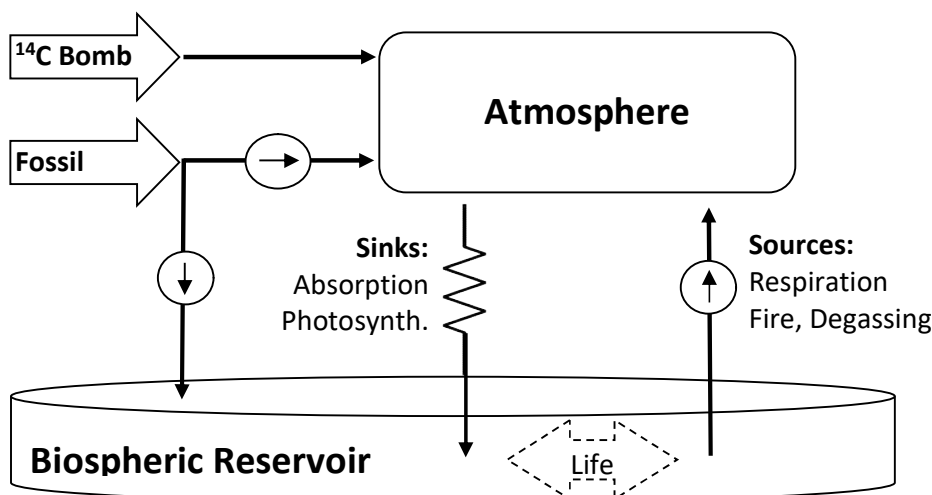


Figure 1: CFR Model. Sources, indicated by the circular arrow symbol, have flows which are not pressure dependant, supplying CO₂ to the atmosphere and reservoir as shown. Sinks have a pressure dependant flow rate, and continuously drain CO₂ from the atmosphere to the biospheric reservoir consisting of land, terrestrial biosphere and surface ocean.

The scheme shown in Fig. 1, termed here the CO₂ Finite Reservoir (CFR) Model is now described. In this diagram CO₂ resides in the atmosphere; its carbon equivalent resides in a finite biospheric reservoir (consisting of land, terrestrial biosphere and surface ocean) whose size is initially determined relative to the atmosphere. The sink processes transfer CO₂ from the atmosphere to the biospheric reservoir, at a rate which is dependant upon the atmospheric partial pressure of CO₂. By analogy with electrical circuits, the sink is drawn as a resistor and can be said to act as a low resistance (or high admittance) drain. This sink flow is compensated by source flow which although having a similar flow rate, has different properties from the sink, in that its flow is unaffected by the differential pressure between origin and destination, the source simply flows. In electrical terms the sources are current-sources; both non-fossil CO₂ input flow and fossil fuel emission input flow having these properties.

Atmospheric CO₂: A finite reservoir model reproduces 14C / 13C over two centuries and indicates the fossil-fuel anthropogenic contribution.

Fossil-fuel emissions divide into two immediate destinations, a flow direct to the atmosphere and a flow direct to the reservoir. The direct flow to the reservoir represents fossil fuel emissions which fail to mix into the atmosphere but are quickly reabsorbed. The deceptive simplicity of the overall scheme is not arbitrary. It is fully detailed in Appendix 1, where it is shown that a single drain and source can represent the bulk effect of any number of different absorption and emission processes. This model is validated using ¹⁴C and ¹³C as trackers in the following section which, offer very good agreement with real-world observations over hundreds of years. The author suggests this simple approach has been overlooked because of an emphasis on complex equilibrium perturbation models rather than considering absolute flows and their intrinsic, inherent properties.

3. Atmospheric Radiocarbon

The most abundant isotope of atmospheric carbon is ¹²C, while around 1 percent is ¹³C and around 1 part in 10¹² is ¹⁴C. Samples of wood, charcoal etc, can provide an historical record of the atmospheric concentration of ¹⁴C and ¹³C, as carbon becomes embedded in the sample. However ¹⁴C and ¹³C exhibit very different properties; with ¹⁴C undergoing radioactive decay with a half-life of 5700 +/-30 years (Kutschera, W., 2013). In contrast both ¹³C and ¹²C are radioactively stable. Fossil fuels, being hundreds of millions of years old, contain virtually no ¹⁴C as it has already radioactively decayed, even beyond the so called "radiocarbon barrier" limit of radiocarbon dating. The combustion of fossil fuels therefore releases virtually ¹⁴C free CO₂ into the atmosphere diluting the ¹⁴C atmospheric concentration, a process known as the "Suess Effect" (Suess 1955). This dilution has been measured in archived tree-ring samples (Stuiver & Quay 1981). However, Stuiver observed that the dilution was only 32% of the expected value and he proposed the reduction should be accounted for by using a "¹⁴CO₂/CO₂ attenuation factor". The CFR model described here provides good agreement with observed ¹⁴C without having to explicitly introduce an attenuation factor, since the factor is implicit in the model.

By contrast with ¹⁴C, the content of ¹³C in fossil fuels is reduced by just a few percent compared to background levels of ¹³C. This reduction is due to fractionation, arising because ¹³C atoms are slightly larger and heavier than ¹²C, and their corresponding reaction rates are slightly slower. During the conversion of atmospheric CO₂ to carbon within the sample, fractionation reduces the relative presence of ¹³C. Therefore, as combustion of fossil-fuels adds CO₂ molecules to the atmosphere the ¹³C concentration falls, in a similar but much less pronounced way than for ¹⁴C.

Before 1900 the ¹³C/¹²C ratio had remained remarkably constant over the previous 10,000 years; its value was maintained to within +/- 0.1‰. However, since 1900 its value has fallen by 2‰. In contrast Δ¹⁴C fell on average by 2‰ each century over the past 10,000 years, occasionally falling by 8‰ in one century. Yet it too has also shown a sudden steeper fall between 1900 and 1950 of 25‰ in only 50 years. Therefore ¹³C and ¹⁴C have both shown exceptional falls since 1900. It is tempting to attribute these falls exclusively to fossil fuel combustion. However, careful analysis shows that although fossil fuel combustion is a significant contributor it is not the only factor. Unfortunately in the case of ¹⁴C the situation becomes further complicated since, from 1950 onwards, the atmospheric ¹⁴CO₂ content almost doubled because of atomic weapons atmospheric tests carried out between 1955 and 1975, a phenomena known as the "bomb pulse". Analysis of the subsequent reduction in ¹⁴C sheds light on the mechanisms of absorption of CO₂. An absorption rate which is proportional to excess pressure is expected to give an exponential shape to the decreasing pulse, and indeed the fall of the bomb pulse (Fig. 3) was initially

Atmospheric CO₂: A finite reservoir model reproduces 14C / 13C over two centuries and indicates the fossil-fuel anthropogenic contribution.

exponential. However, its falling shape has changed and although the atmospheric ¹⁴C level is just above zero per mil (‰) in 2020 it now exhibits a linear rate of decrease. Levin (2009) has discussed this shape and calculated a theoretical reduction rate due to CO₂ff dilution alone as 12-14 ‰ per year which she suggested "is partially compensated by ¹⁴CO₂ release from the biosphere, industrial ¹⁴CO₂ emissions and natural ¹⁴C production." Here we suggest that release from the biosphere, by which we mean land, terrestrial biosphere and surface ocean is the most significant factor, with the latter two "compensating" effects from Levin's paper (industrial ¹⁴CO₂ emissions and natural ¹⁴C production) being relatively small (Svetlik 2010, Stuiver & Quay 1981). While the effects of CO₂ff act to reduce the equilibrium value, the effect of biospheric inflow can act in the opposite direction, raising the atmospheric equilibrium value depending upon the reservoir size. For a reservoir which is infinite, its ¹⁴C activity, by definition, must remain constant at background level, and hence inflow from the reservoir could never raise the atmospheric ¹⁴C equilibrium level; therefore an inflow from an infinite reservoir would serve only to accelerate the fall of the pulse shape to its previous equilibrium value. However, if the reservoir is finite, as the reservoir fills its ¹⁴C level will increase and the reservoir and atmosphere must then equilibrate at a higher value than the original background value. This paper shows that the combined effects of a) a finite reservoir and b) Suess dilution, can produce the precise temporal shape of the atmospheric ¹⁴C activity curve. The above qualitative description is quantitatively embedded in the CFR model. The results shown below indicate its output between 1820 to the present day for both ¹⁴C and ¹³C including during the period of the ¹⁴C bomb pulse.

4. Results

Appendix B describes the CFR model and the calculation of sink and source flow together with isotopic mixing. The graphs shown below use the optimum solutions for the model, defined as the minimum value of the product of the standard deviations for all three graphs, i.e. between experimental and observed value σ_1 for $\Delta^{14}\text{C}$ 1820 to 2020 using INTCAL20 and SHCAL20, σ_2 for $\Delta^{14}\text{C}$ 1960 to 2020 $\Delta^{14}\text{C}$ Hua and σ_3 for $\delta^{13}\text{C}$ 1820 to 2020 NOAA Paleo. The cube root of the resulting product ensures its units are still in mill, hence

$$sd = (\sigma_1 \times \sigma_2 \times \sigma_3)^{1/3}$$

$$\sigma_j = \sqrt{1/n \sum (\text{obs}_i - \text{calc}_i)^2}$$

The optimum solution was found by variation of 7 parameters, fossil-fuel inflow partitioning, nuclear bomb yield, atmospheric lifetime, reservoir size, initial value of $\delta^{14}\text{C}$, $\delta^{13}\text{C}_\text{N}$, $\delta^{13}\text{C}_\text{F}$. Only one constant was used, atmospheric capacity = 2.124 ppm GTC⁻¹ (Ballantyne 2012). The parameters used in the minimisation are listed below, with the determined values being shown in brackets.

The CFR model tracks the ¹⁴CO₂ and ¹³CO₂ using the formulae presented in Appendix A and B, implemented as iterative recurrence relationships shown in Appendix C.

a) Fossil-fuel Inflow Partitioning ($ff_{\text{atmos}} = 49\%$, $ff_{\text{res}} = 51\%$)

This parameter specifies the proportion of fossil-fuel inflow which is delivered to the atmosphere and reservoir respectively. Their sum is unity, meaning all reported fossil-fuel emissions are used. Figures (2-4) depend on this parameter. Recent studies of daytime releases of ¹⁴CO₂ in the vicinity of nuclear power plants have reported significant ¹⁴CO₂ uptake (Masakazu O. et al. 2016). A ¹⁴C study of urban grasses near a major highway in Paris, France, reported plants stored up to 13% of fossil-fuel

Atmospheric CO₂: A finite reservoir model reproduces 14C / 13C over two centuries and indicates the fossil-fuel anthropogenic contribution.

carbon (Lichtfouse 2005). This may also be compared with the airborne fraction which is reported as around 0.44 and is defined as "The fraction of total CO₂ emissions (from fossil fuel and land use change) remaining in the atmosphere". IPCC (Ciais, P. et al, 2013). Therefore, the percentage of fossil-fuel emissions being absorbed by nearby plants or by water prior to global mixing, as given by ff_{atmos} , do not appear to be unreasonable.

b) Nuclear bomb yield ($Y_b = 0.75$)

This constant provides the amount of ¹⁴CO₂ per megaton of nuclear bomb explosive power in units of background ¹⁴C level. Only Fig. 3 is dependent on Y_b . The values of annual bomb size were taken from data reference UNSCEAR 2000. In practice the optimum fit was obtained when the releases were delayed by one year in order to allow for its propagation. The uncertainty regarding bomb yield has been discussed by Hesshaimer, V. et al. 1994.

c) Time constant ($\tau_a = 15.0$ yrs)

This constant represents a bulk parameter describing the global absorption processes and their drain on the atmosphere. Figures 2-5 depend on τ_a . Values of this order were first deduced in 1957 (Revelle & Suess 1957, Arnold & Anderson 1957), with both papers using a linear description. However these papers subsequently were criticised for overlooking the effects of ocean vertical mixing. See Discussion below.

d) Reservoir Size ($R_{CO_2} = 6.49$)

This constant represents the size of the reservoir relative to the atmosphere itself. Figs 2-5 depend on R_{CO_2} . The uncertainty in the relative size of the shallow ocean layer has been discussed by Hesshaimer et al 1994. Just as with the other parameters, the CFR determines this reservoir size as being the value providing the best fit. Previous attempts by the author to use an infinite reservoir size resulted in a slightly worse fit, especially in the tail of the "bomb pulse", since the flow of CO₂ into an infinite reservoir does not, by definition, change its ¹⁴C/¹²C ratio, (irrespective of its level of Suess dilution) and hence the system attains an equilibrium value which is not found in practice.

e) ¹⁴C Pre-industrialisation background ($\delta^{14}C = - 3.4$ ‰)

This value was entered as the reservoir and atmospheric values as the initial level of ¹⁴C in AD0. It remains unchanged until fossil fuel emissions start to dilute the atmosphere at the start of industrialisation.

f) ¹³C Pre-industrialisation background and fossil fuel levels ($\delta^{13}C_B = - 6.7$ ‰, $\delta^{13}C_F = - 21.7$ ‰)

These parameters represent the general ¹³C atmospheric values before industrialisation and that for fossil-fuel emissions, respectively. Values have been reported of $\delta^{13}C_N = -6.5$ ‰ for pre-industrialisation (Rubino, M et al 2013) and $\delta^{13}C_F = -23$ ‰ for coal, (Stuiver M & Polach H A. 1977), this being the major global fossil fuel during the period. However lower values have been reported for diesel and petroleum (-29‰) and for natural gas (-37‰) (Bush et al 2007), suggesting the figure of $\delta^{13}C_F$ is a little high. The precise cause of the discrepancy between the value determined here by the CFR model and the reported values is not clear.

The model was run from 0AD to 2020AD, with results from 1820AD onwards shown below for $\Delta^{14}C$ in Figs. 2-3 and $\delta^{13}C$ in Fig. 4. The resulting standard deviation σ in mills is indicated in each graph caption.

Atmospheric CO₂: A finite reservoir model reproduces ¹⁴C / ¹³C over two centuries and indicates the fossil-fuel anthropogenic contribution.

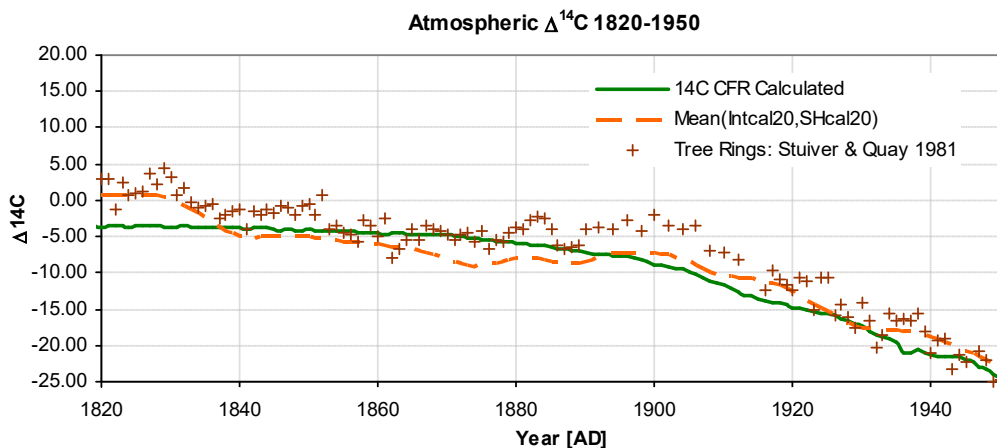


Figure 2: Atmospheric $\Delta^{14}\text{C}$ 1820-1950. CFR calculated: (solid line). Mean (Intcal20, SHcal20) (dashed line) $\sigma_{1820-1950} = 2.1\text{‰}$ Tree-rings: Stuiver and Quay 1981 NH (Crosses).

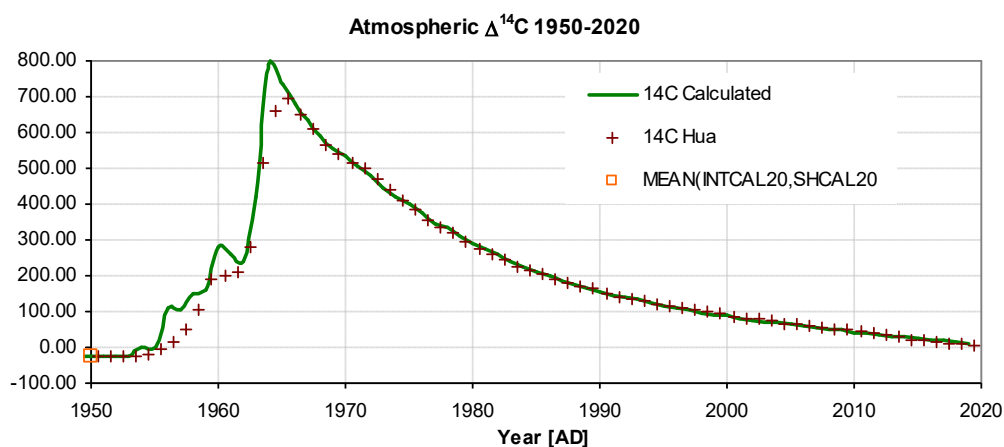


Figure 3. Atmospheric $\Delta^{14}\text{C}$ 1950-2020. CFR calculated values: (solid line). Collated: Hua 2021 (crosses), Mean SHCAL20 and INTCAL20 (Square) $\sigma_{1966-2020}=4.7\text{‰}$. The shape and fit of the tail of the pulse is particularly affected by the finite reservoir size (see text).

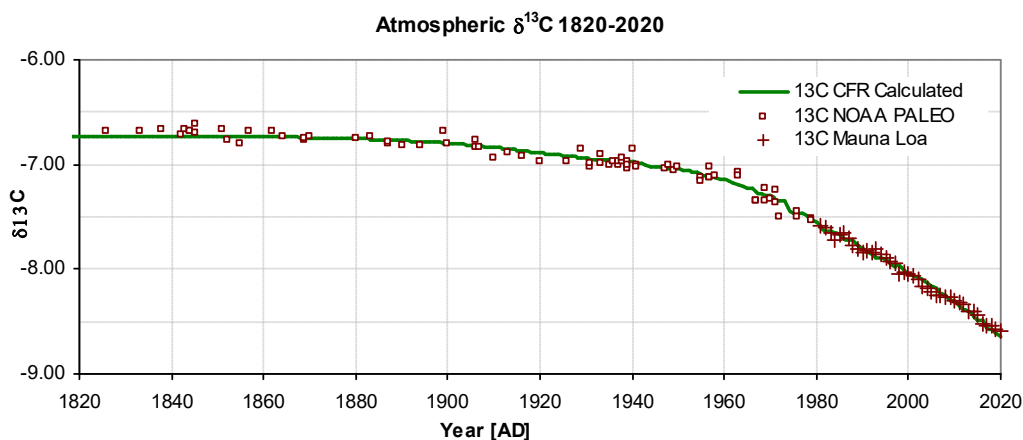


Figure 4. Atmospheric $\delta^{13}\text{C}$ 1820-2020. CFR calculated values (solid-line), Observed values: NOAA Paleo (squares), Mauna Loa (crosses) $\sigma_{1820-2020} = 0.05\text{‰}$.

Atmospheric CO₂: A finite reservoir model reproduces 14C / 13C over two centuries and indicates the fossil-fuel anthropogenic contribution.

The graphs show excellent agreement between the CFR model and the observed global measurements. In Fig. 2, prior to the atomic bomb, the reduction of $\Delta^{14}\text{C}$ can be seen due to partial dilution from fossil fuel combustion, its value fits the observations well. Although such dilution is still present after 1950 it is not apparent because of the greater magnitude of the bomb pulse, Fig. 3. The CFR model inherently takes account of dilution, returning accurate representations for the pre-bomb, bomb and post-bomb pulse shape (Hua 2021), without the need for Stuiver's " $^{14}\text{CO}_2/\text{CO}_2$ attenuation factor".

It has already been mentioned that, in the case of ^{14}C , this factor could indicate the presence of a natural source. Similarly it can be readily shown that the decrease in $\delta^{13}\text{C}$ in Fig 4 is not just due to fossil-fuel dilution alone but also arises from dilution by a natural ^{13}C inflow. Re-plotting the data from Fig 4 into Fig 5 using an x-axis of CO₂ in ppm rather than time, shows that an increase in CO₂ level solely driven by fossil-fuel inflow should create a steeper negative slope than that seen. For example, taking fossil-fuel as $\delta^{13}\text{C} = -19.6\text{‰}$, and the atmospheric ^{13}C value of $\delta^{13}\text{C} = -6.9\text{‰}$ when the atmospheric mixing ratio was 300ppm, the expected downward slope calculated from Eq A2 is 0.033, rather than the observed value of 0.016, Fig 5. This discrepancy resembles Stuiver's "attenuation factor" but this time applied to $\delta^{13}\text{C}$. The reason for the weakening of the ^{13}C dilution is the same as in the case of ^{14}C ; the inflow of CO₂ from the reservoir has a greater isotopic concentration than that from fossil fuel combustion alone.

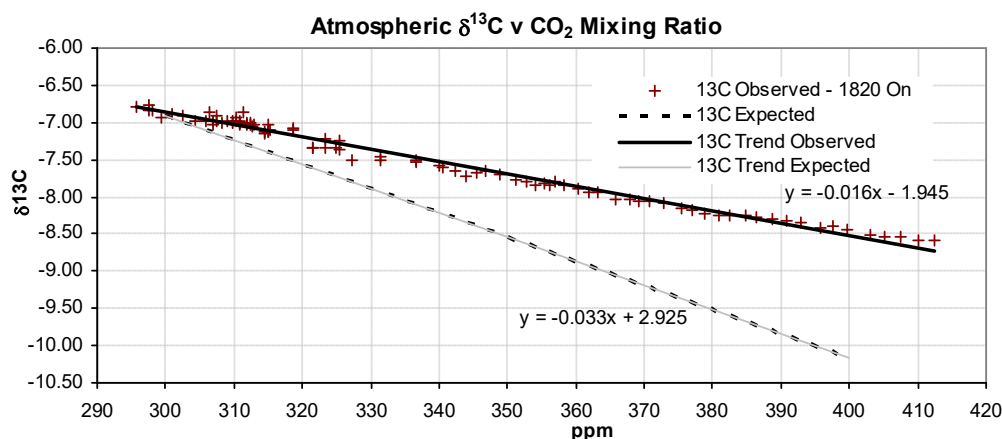


Figure. 5. $\delta^{13}\text{C}$ v CO₂ mixing ratio (ppm) showing the trend-line for observed and expected values.

In addition to offering good agreement with observations, the CFR model offers the ability to track the fossil level and the natural level individually in both atmosphere and reservoir. The results in Fig. 6 shows the CFR calculated curve and the experimentally observed data of Fig 4. mapped using Eq. (A6) with the fixed values of $\delta^{13}\text{C}_F$ and $\delta^{13}\text{C}_B$ (Quirk T. 2021). The results indicate a departure from accepted wisdom, with contributions to atmospheric CO₂ originating from both fossil and non-fossil inflow occurring in approximately equal proportions as indicated by the approximately equal slope of each curve.

Atmospheric CO₂: A finite reservoir model reproduces 14C / 13C over two centuries and indicates the fossil-fuel anthropogenic contribution.

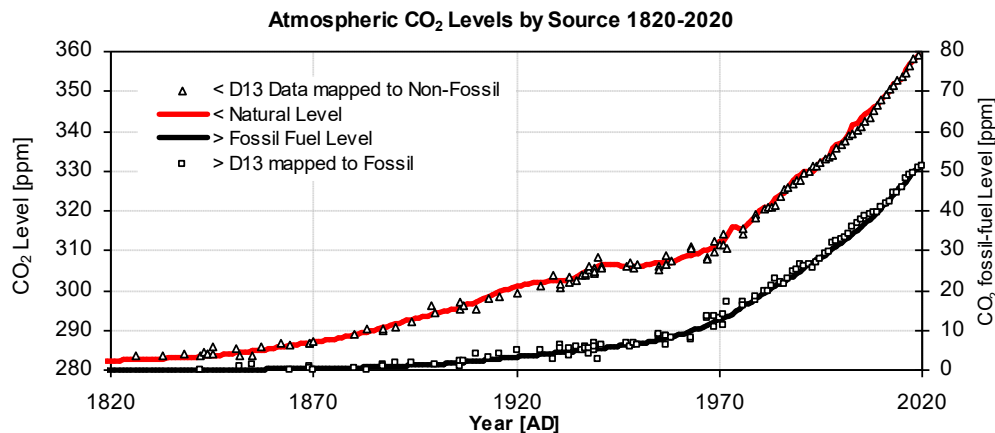


Figure 6. Atmospheric Levels. CFR calculated (fossil black-line, non-fossil red-line). Measured values mapped via Eq.(A6) using $\delta^{13}C_F$, $\delta^{13}C_B$ to fossil (square) and non-fossil (triangle).

The results are tabulated for fossil and non-fossil contributions in Table 1 showing that the fossil-fuel airborne fraction of atmospheric CO₂ has remained fairly constant irrespective of the period, with 23% to 24% remaining in the atmosphere, while 76% to 77% has been absorbed in the reservoir. However, the atmospheric increase due to fossil fuels from the past 270 years is 38%, increasing to 48% from the past 11 years. This increase can also be seen by examination of Fig 6, where the slope of the fossil fuel contribution is becoming steeper with time. During the post-industrial period from 1750 to 2020, 52 ppm of the total CO₂ atmospheric concentration is due to fossil fuels, which corresponds to 13% of the total atmospheric CO₂ at 2020 level. These figures include the re-emission of CO₂ back from the biospheric reservoir to the atmosphere.

Table 1: Cumulative CO₂ Flows and Storage over various periods.

Duration (inclusive)	1750-2020	1900-2020	2010-2020	
Number of Years	269	120	10	
1 Fossil-fuel CO ₂ Input	218	212	50	ppm
2 Fossil-fuel CO ₂ Outflow	166	162	39	ppm
3 Atmos. CO ₂ Increase due to Fossil Fuels (1-2)	52	51	11	ppm
4 Atmos. CO ₂ Increase due to Non-Fossil Fuels	83	66	12	ppm
5 Atmos. CO ₂ Increase during period (3+4)	135	117	24	ppm
6 Atmos. CO ₂ Increase due to Fossil-fuels (3/5)	38	43	48	%
7 Atmos. CO ₂ Increase due to Natural Inflow (4/5)	62	57	52	%
8 Fossil-fuel CO ₂ being Stored (2/1)	76	76	77	%
9 Fossil-fuel CO ₂ to Atmos. (Airborne Fraction) (3/1)	24	24	23	%
10 Increase rel to final total atmos. CO ₂ (3)/C _A *	13	12	3	%
11 Average Source Flow	20.41	22.19	26.80	ppm/yr
12 Average Sink Flow	20.31	22.09	26.66	ppm/yr

* The CO₂ atmospheric mixing ratio in 2020, C_A = 412.44 ppm.

5. Discussion

Care should be taken when making direct comparisons of flow data from Table 1 (rows 11, 12), with other sources because of differing flow definitions. For example, the Global Carbon Budget (GCB) reports that for the period 2010 to 2019 the mean value of land sink is 3.4GtCyr⁻¹ and ocean sink is 2.5GtCyr⁻¹; giving a total sink of 5.9 GtCyr⁻¹ corresponding to 2.77ppm. (Friedlingstein P. et al, 2020). For the same

Atmospheric CO₂: A finite reservoir model reproduces 14C / 13C over two centuries and indicates the fossil-fuel anthropogenic contribution.

period the CFR model has a mean value of 27ppm, ten times greater. However, closer inspection reveals that GCB figures represent the perturbation-nett flow, accounting for nett CO₂ movements. In the CFR model emissions do not cancel either by day or geographically. Plants may emit by night and absorb by day, oceans may absorb where and when cold and emit where and when warm; CFR accounts for these effects separately hence its figures exceed those of the GCB. The CFR values reflect their definitions and are based upon absolute figures which are not temporally or spatially averaged.

According to popular wisdom, fossil fuel emissions account for virtually all of the post-industrial atmospheric increase. IPCC reports "the increase in CO₂ emissions... are the dominant cause of the observed increase in atmospheric CO₂ concentration." P467 WG1AR5 (Ciais, P. et al, 2013). EPA 2020 reports "While CO₂ emissions come from a variety of natural sources, human-related emissions are responsible for the increase that has occurred in the atmosphere since the industrial revolution" (EPA 2020). In contrast, Fig. 5 shows two sources, fossil fuel and natural which sum to the total CO₂ value. Both the $\delta^{13}\text{C}$ and $\Delta^{14}\text{C}$ evidence, as in the above examination of Figs 5 & 6, directly reveals the existence of a further natural source. The existence of a sizeable inflow, rejected by many, is a consequence of the idea of a drain, because absolute flows, not perturbed-nett-flows, are used in the model. Therefore, because there is a sink flow, there must also be a restoring source flow of similar magnitude to approximately restore the balance in the level of atmospheric level of CO₂. It is this absolute source which has increased since industrialisation, preventing that fall in $\delta^{13}\text{C}$ which would have occurred solely from fossil fuel combustion.

Variation in natural source flows are known to have occurred during the deglaciation between 16ka and 12ka, when changes in global temperature accompanied century-scale variations in CO₂ and $\delta^{13}\text{C}$ (Basuka et al 2014, Bengtson et al 2020, Marcott et al., 2014). This reinforces the view that changes in natural CO₂ source production should not be overlooked when accounting for atmospheric CO₂ fluctuations, especially when accompanied by a global temperature rise.

A frequent criticism of studies using CO₂-lifetime and the bomb-pulse is that "a single, characteristic atmospheric lifetime is not applicable to CO₂" (Ciais et al. 2013). Other criticisms include; "the different behaviour of a pulse of carbon isotope compared with a ¹²C pulse" (regarding seawater absorption), the effect of the Revelle factor and fractionation in CO₂ seawater absorption kinetics, "¹²C being dislodged by ¹³C", and what is termed "isotopic swapping" (Harvey L.D. 2000, Archer D. 2009, Joos F. 1994). This paper shows that such esoteric processes do not need to be invoked. On the contrary, a combination of a single time-constant in the rate equation, a finite biospheric reservoir together with the classic mixing equations can accurately describe the $\Delta^{14}\text{C}$ from 1820 to 2020, including the bomb pulse, and also ¹³C.

The simultaneous agreement of the three graphs, Fig. 3, ($\Delta^{14}\text{C}$ pre-bomb), Fig. 4 ($\Delta^{14}\text{C}$ post-bomb) and Fig. 5 ($\delta^{13}\text{C}$ 1820-2020) showing little difference between the measured and calculated data is highly significant.

6. Conclusion

This study introduced a method of describing global absolute atmospheric CO₂ flows between an idealized atmosphere and a finite reservoir, employing a classic rate ODE. The model provides a high degree of agreement with observed values of ¹⁴C and ¹³C over periods of 200 years, it accurately describes the temporal shape of the nuclear weapons bomb pulse and it resolves the long-running question of multiple atmospheric CO₂ residence times, showing that a single time-constant can be

Atmospheric CO₂: A finite reservoir model reproduces 14C / 13C over two centuries and indicates the fossil-fuel anthropogenic contribution.

usefully applied to atmospheric CO₂. It also shows that a finite biospheric reservoir with a CO₂ capacity around 6 times that of the atmosphere can accurately describe $\Delta^{14}\text{C}$ over 200 years, including during the bomb pulse. The model produces values for the airborne fraction of fossil fuel CO₂ of around 24%; these are lower than the conventionally accepted figure of 44% (Ciais, P. et al, 2013), which implies a higher proportion of fossil-fuel CO₂ is being absorbed in the biosphere than otherwise reported. However, the CFR model also shows an increasing "natural" level caused by CO₂ inflow from the biosphere, thereby providing evidence of a process beyond human-control, making mitigation of CO₂ levels if desired, more difficult. This paper shows that the global climate, despite its apparent complexity, can be simplified using certain assumptions relating to its flow properties. Just as the concepts of conservation of momentum and energy provide a top-down simplification of physical processes and interactions, the CFR model thus avoids the necessity to analyse individual processes. This top-down approach yields an insight which is not provided by complex climate models.

7. Acknowledgments

I would like to thank my colleagues Dr. Andrew Layfield (Physicist), City University, Hong Kong, and Dr. Michael Oates (Geologist) of Barrow-upon-Humber, UK for their detailed comments and proof reading. The author would like to thank and acknowledge all the data providers indicated in "Data References", without whom this work could never have been carried out.

Atmospheric CO₂: A finite reservoir model reproduces 14C / 13C over two centuries and indicates the fossil-fuel anthropogenic contribution.

APPENDIX

Appendix A. Notes on Isotopic Mixtures and Radiocarbon Levels

Dalton's "Law of Partial Pressures" indicates that, when two gases having partial pressure P_A and P_B and concentration R_A and R_B , are mixed, then the total pressure, P_T of the mixture will be given by

$$P_T = P_A + P_B$$

and its concentration R_M of the mixture or model is

$$R_M = (R_A P_A + R_B P_B) / P_T$$

Note: If the isotopic amount is described by an offset scale e.g. $R = (m \cdot \delta a + c)$ the above becomes

$$(m \delta m + c) P_T = (m \delta a + c) P_A + (m \delta b + c) P_B$$

which after rearranging gives equations of similar form, i.e.

$$\delta_m P_T = \delta a P_A + \delta b P_B \quad (A1)$$

$$\delta_m = (\delta a P_A + \delta b P_B) / P_T \quad (A2)$$

Conversely, for a mixture of total pressure, P_T , whose concentration is δ_m , given the concentration of its two constituents δa and δb , the pressure of the constituent P_A , is given by (Quirk T. 2021)

$$P_A = P_T (\delta_m - \delta b) / (\delta a - \delta b) \quad (A3)$$

Conventionally $\delta^{14}C$ is defined as an offset scale whose value is zero when A_s , the specific activity of the atmosphere or reservoir is equal to A_{abs} , the absolute specific standard, with both being in units of Bq per unit mass of carbon. Hence we may write

$$A = \delta^{14}C + 1 = (A_s / A_{abs})$$

where A refers to the relative specific ^{14}C activity. Thus A contains no allowance for radioactive decay or fractionation. For the mixture M obtained by mixing natural N and fossil fuel derived F components we may write using Eq. A2 for A_M and $\delta^{13}C_M$

$$A_M = (A_N P_N / P_T) - 1 \quad (A4)$$

$$\delta^{13}C_M = (\delta^{13}C_F P_F + \delta^{13}C_N P_N) / P_T \quad (A5)$$

bearing in mind that $A_F = 0$. The inverse for $\delta^{13}C_M$, used in Fig. 6 to map from observed atmospheric values of δ^{13} to CO₂ levels by source from Eq. A(3) is

$$P_N = P_T (\delta^{13}C_M - \delta^{13}C_F) / (\delta^{13}C_N - \delta^{13}C_F) \quad (A6)$$

Fractionation

It is desired to compare values of A_M with collated measured values of $\Delta^{14}C$. However

Atmospheric CO₂: A finite reservoir model reproduces 14C / 13C over two centuries and indicates the fossil-fuel anthropogenic contribution.

$\Delta^{14}\text{C}$ incorporates a fractionation correction to "translate the measured activity to the activity the sample would have had if it had been wood" (Lund 2011) and is a function of $\delta^{13}\text{C}$. Therefore a fractionation correction must be applied to A_M , where δ^{13} for wood is taken as -25‰, given by

$$\Delta^{14}\text{C}_M = A_M \cdot \left\{ \frac{(1 + \delta^{13}\text{C}_W)}{(1 + \delta^{13}\text{C}_M)} \right\}^2 - 1$$

This formula decreases the values by around 35‰ compared to the values for A_M .

Age Correction

Sample age correction, common in radiocarbon calculations, is not included in the CFR or the definition of $\Delta^{14}\text{C}$. The ¹⁴C half-life of 5700±30 years (Kutschera, W., 2013) translates to a decay of around 2% over the period 1820 to 2020. However, the steady level of stratospheric ¹⁴C production roughly balances the amount of ¹⁴C decay since the two are in approximate equilibrium, providing a buffering effect. Disregarding ¹⁴C decay introduces an error at most in the low percentage region and probably considerably smaller and is regarded as negligible. Therefore neither ¹⁴C decay nor natural stratospheric ¹⁴C production were included in the CFR model. Values of A were not artificially corrected for ¹⁴C decay before comparison with $\Delta^{14}\text{C}$.

Appendix B. CO₂ Finite Reservoir Model (CFR)

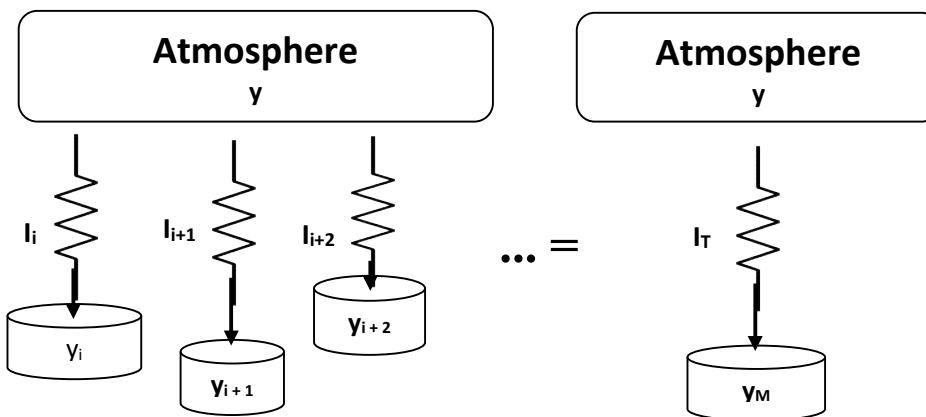


Figure. B1: Multiple Atmospheric Sinks. Multiple sinks are represented by a single bulk value.

We assume each process 'i' creates a flux I_i of CO₂ which depends on the difference between its intrinsic partial pressure, y_i , and the ambient atmospheric level, y , together with a flow constant of proportionality, σ_i , as

$$I_i = \sigma_i (y_i - y) \quad (\text{B1})$$

The constant σ_i represent the admittance of the process, this being the inverse of the resistance. Summing over all processes gives a total flow I_T as

$$I_T = \sum I_i = \sum \sigma_i y_i - y \sum \sigma_i \quad (\text{B2})$$

Writing a bulk admittance, σ_T , as

$$\sigma_T = \sum \sigma_i \quad (\text{B3})$$

Rearranging, the total flow I_T is given in a similar form to Eq. (B1) i.e.

Atmospheric CO₂: A finite reservoir model reproduces 14C / 13C over two centuries and indicates the fossil-fuel anthropogenic contribution.

$$I_T = \sigma_T (y_M - y) \quad (B4)$$

where y_M is an effective mean pressure given by

$$y_M = \Sigma[(\sigma_i y_i)] / \sigma_T \quad (B5)$$

Thus any number of individual processes can be merged using bulk properties as in Fig. B1. The summed flow leaving the atmosphere creates a continuous rate of change of pressure and we may write

$$dy / dt = C_A I_T$$

where $C_A = 2.124 \text{ GTC ppm}^{-1}$ (Ballantyne et al. 2012), is termed here the atmospheric capacity (by analogy with a capacitor or fluid container). Hence the flow I_T results in a rate of change of atmospheric pressure given by

$$dy/dt = (\sigma_T / C_A) (y_M - y) \quad (B6)$$

and the effective pressure constant can be written as

$$\alpha = \sigma / C_A$$

Equation (B6) is a first order ordinary differential equation (ODE). When subject to an additional external flux $q(t)$ such as may occur from the atomic bomb pulse or fossil fuel combustion or other inflows we may add the additional flow to the flow equation, writing

$$dy/dt = \alpha_T (y_M - y) + q(t) \quad (B7)$$

When the flux $q(t)$ is a single impulse delta function $\delta(0)$ occurring at time $t=0$, such as in a single bomb pulse, Eq. (B7) gives

$$y = y_M + H(0) e^{-t/\tau} \quad (B8)$$

where $H(0)$ is the unit step function. Equation (B8) may be verified by differentiation and substitution into (B5), bearing in mind that the derivative of a step function is a delta function. The substitution directly provides the value of the exponential decay time constant τ as

$$\tau = 1 / \alpha_T \quad (B9)$$

Hence Eq. (B6) may be rewritten as

$$dy/dt = (y_M - y) / \tau \quad (B10)$$

In Fig. 1, the source provides the in-flow, and the summation gives a single value for admittance to out-flow. At equilibrium the atmospheric CO₂ level is static, hence its value is determined by the inflow flow divided by the admittance. It is assumed the admittance of the sources, fire, respiration and degassing are very low and hence their value does not substantially affect the admittance summation and hence, the time constant.

Appendix C: Implementation

We now can use Eq.(B10) to calculate the annual CO₂ drawdown given the annual listings of CO₂ level. The outflow from the atmosphere, y_{n-1}/τ , flows into a reservoir of finite size. Any rising back pressure arising from the filling of the reservoir (termed its carbon potential) is regarded as negligible. The inflow to the atmosphere from the reservoir is calculated as the sum of the above derived outflow and the known increase in atmospheric CO₂ level, but subtracting the inflow of fossil fuels into the atmosphere. Regarding the reservoir, the outflows from the atmosphere is the main inflow to the reservoir, which is supplemented by the direct portion of fossil fuel inflow. The process involves a number of calculations at each iteration. These are

Atmospheric CO₂: A finite reservoir model reproduces 14C / 13C over two centuries and indicates the fossil-fuel anthropogenic contribution.

largely based upon "Dalton's Law of Partial Pressures". The iteration recurrence relationships are:-

$$A_{OUT}[i] = A_{CO2} [i] / tc$$

$$A_{IN}[i] = A_{OUT} [i] + A_{CO2} [i] - A_{CO2} [i-1] - FF_{ATMOS} [i]$$

$$A_{14}[i] = (A_{14} [i-1].A_{CO2} [i-1] + A_{IN} [i-1].R_{14}[i-1] - A_{OUT}[i-1]. A_{14}[i-1] + B_{14}[i-1]) / A_{CO2} [i]$$

$$R_{14}[i] = (R_{14} [i-1].R_{CO2} [i-1] - A_{IN} [i-1].R_{14}[i-1] + A_{OUT}[i-1]. A_{14}[i-1]) / R_{CO2} [i]$$

$$R_{CO2}[i]=R_{CO2}[i-1]+A_{OUT}[i] - A_{IN}[i]$$

$$A_{FF}[i] = (A_{FF} [i-1].A_{CO2} [i-1] + A_{IN} [i-1].R_{FF} [i-1] - A_{OUT}[i-1].A_{FF}[i-1] + F_{ATMOS}[i]) / A_{CO2} [i]$$

$$R_{FF}[i] = (R_{FF} [i-1].R_{CO2} [i-1] - A_{IN} [i-1].R_{FF} [i-1] + A_{OUT}[i-1].A_{FF}[i-1] + F_{RSVR}[i]) / R_{CO2} [i]$$

$$FL[i] = A_{CO2}[i] . A_{FF}[i], NL[i] = A_{CO2}[i] - FL[i]$$

$$\delta^{13}C = \delta^{13}C_{FF} . A_{FF} + \delta^{13}C_N (1 - A_{FF})$$

$$\Delta^{14}C = (A_{14} - 1)$$

$$\text{Initial Conditions: } A_{IN} [0] = A_{OUT} [0] , A_{14} [0] = 1 , R_{14} [0] = 1 , A_{FF}[0] = 0 , R_{FF}[0] = 0$$

where:

A_{OUT} is the atmospheric outflow, A_{CO2} is the atmospheric CO₂ mixing ratio, A_{IN} is the atmospheric inflow, R_{CO2} is the reservoir CO₂ mixing ratio, R_{FF} is the fossil fuel level in the reservoir, R_{14} is the f¹⁴C level in the reservoir, F_{RSVR} is the Fossil fuel CO₂ mixing ratio in the reservoir, F_{ATMOS} is the Fossil fuel inflow to the atmosphere, F_{RSVR} is the fossil fuel inflow to the reservoir, A_{14} is the f¹⁴C level in the atmosphere, B_{14} is the total ¹⁴C production due to atomic weapons testing $\Delta^{14}C$ is the ¹⁴C/¹²C ratio and $\delta^{13}C$ is the ¹³C/¹²C ratio and the square brackets "[]" refer to the value at each iteration.

The model can be downloaded as a Microsoft Excel Spreadsheet from <https://www.geomatix.net/download.htm>.

References

Archer, D et al. 2009. Atmospheric lifetime of fossil fuel carbon dioxide. *Annu. Rev. Earth Planet. Sci.*, 2009. 37:117–134.

Arnold J.R. & Anderson E.C. 1957. The Distribution of Carbon-14 in Nature. *Tellus IX 1957*.

Ballantyne, A. P et al. 2012. Increase in observed net carbon dioxide uptake by land and oceans during the last 50 years. *Nature*, 488, 70–72.

Bauska et al. 2014 Carbon isotopes characterize rapid changes in atmospheric carbon dioxide during the last deglaciation. *PNAS* | March 29, 2016 | vol. 113 | no. 13 | 3465–3470

Bengston et al. 2020 Lower oceanic $\delta^{13}C$ during the last interglacial period compared to the Holocene. *Clim. Past*, 17, 507–528, <https://doi.org/10.5194/cp-17-507-2021>, 2021.

Bush S.E. et al 2007. Sources of variation in d¹³C of fossil fuel emissions in Salt Lake City, USA , *Applied Geochemistry* 22 (2007) 715–723

Ciais, P. et al, 2013. Carbon and Other Biogeochemical Cycles. Chapter 6. *Climate Change 2013: The Physical Science Basis*. [Stocker et. al] WG1 AR5 IPCC 2013.

Environmental Protection Agency USA 2020. Accessed 23 Jan 2022 <https://www.epa.gov/ghgemissions/overview-greenhouse-gases>.

Atmospheric CO₂: A finite reservoir model reproduces 14C / 13C over two centuries and indicates the fossil-fuel anthropogenic contribution.

Friedlingstein P. et al, 2020. Global Carbon Budget 2020, *Earth Syst. Sci. Data*, 12, 3269–3340, <https://doi.org/10.5194/essd-12-3269-2020>, 2020

Harvey Danny LD 1960, *Global Warming: The Hard Science*, Pearson Education Limited, UK. ISBN 0582-38167-3

Hesshaimer, V. et al 1994. Radiocarbon evidence for a smaller oceanic carbon dioxide sink than previously believed. *Nature*, 370(6486), 201–203. doi:10.1038/370201a0

Hua Q. et al. Atmospheric Radiocarbon For The Period 1950–2019, *Radiocarbon* Vol 0 Nr00 2021. Submitted. Private Communication

Joos F. 1994. , Imbalance in the Budget, *Nature* Vol 370 21July 1994

Joos, F., et al. 2013. Carbon dioxide and climate impulse response functions for the computation of greenhouse gas metrics: A multi-model analysis. *Atmos. Chem. Phys.*, 13, 2793–2825

Kutschera, W., (2013) Applications of accelerator mass spectrometry. *International Journal of Mass Spectrometry* 349, 203-218.

Levin I. et al. 2010 Observations and modelling of the global distribution and long-term trend of atmospheric 14CO₂. *Tellus B*, 62: 26-46 2010.

Lichtfouse, E. et al. 2005. 14C of grasses as an indicator of fossil fuel CO₂ pollution. *Environmental Chemistry Letters*, 3(2), 78–81. 2005. doi:10.1007/s10311-005-0100-4

Marcott A S et al., 2014. Centennial-scale changes in the global carbon cycle during the last deglaciation. *Nature*, Vol 514, 30October 2014

Masakazu O. et al. 2016. Impacts of C-uptake by plants on the spatial distribution of 14C accumulated in vegetation around a nuclear facility, *Journal of Environmental Radioactivity*, Volumes 162/163, 2016, <https://doi.org/10.1016/j.jenvrad.2016.05.032>.

Quirk T. 2021 Suggested method using inversion formulae for d13C. Private Communication 2021

Rubino, M et al 2013. A revised 1000 year atmospheric δ13C-CO₂ record from Law Dome and South Pole, Antarctica. *Journal of Geophysical Research: Atmospheres*, 118(15), pp.8482-8499. 2013

Strassmann K. M. & Joos F. 2018. The Bern Simple Climate Model (BernSCM) v1.0: an extensible and fully documented open-source re-implementation of the Bern reduced-form model for global carbon cycle–climate simulations.

Stenström K. E. 2011. A guide to radiocarbon units and calculations, Lund University, Department of Physics, Division of Nuclear Physics. Sweden. 201111

Revelle, R & Suess H, 1957. Carbon Dioxide Exchange Between Atmosphere and Ocean and the Question of an Increase of Atmospheric CO₂ during the Past Decades. *Tellus IX*(1957).1

Stuiver, M. & Quay, P.D. 1981. Atmospheric ¹⁴C changes resulting from fossil fuel CO₂ release and cosmic ray flux variability. *Earth and Planetary Science Letters*, 53 (1981) 349-362

Stuiver M & Polach H A. 1977 Discussion: Reporting of 14C Data, *Radiocarbon*, Vol19 No 3 1977 P355-363

Atmospheric CO₂: A finite reservoir model reproduces 14C / 13C over two centuries and indicates the fossil-fuel anthropogenic contribution.

Stuiver et al. 1998 "INTCAL98 RADIOCARBON AGE CALIBRATION, 24,000-0 cal BP", RADIOCARBON, VOL. 40, No. 3, 1998, P.1041-1083

Suess, H.E. 1955 Radiocarbon concentration in modern wood. Science 122, 415.

Svetlik I. 2010 Estimation of Long-Term Trends in the Tropospheric 14CO₂ Activity Concentration. Proceedings of the 20th International Radiocarbon Conference, edited by A J T Jull, RADIOCARBON, Vol 52, Nr 2–3, 2010, p 815–822

Zhu Z., et al. 2016 Greening of the Earth and its drivers. Nature Clim Change 6, 791–795 (2016). <https://doi.org/10.1038/nclimate3004>

Data References

1. Institute for Atmospheric and Climate Science (IAC), CO₂ Mean Global AD0 to AD2014 ftp://data.iac.ethz.ch/CMIP6/input4MIPs/UoM/GHGConc/CMIP/yr/atmos/UoM-CMIP-1-1-0/GHGConc/gr3-GMNHSH/v20160701/mole_fraction_of_carbon_dioxide_in_air_input_4MIPs_GHGConcentrations_CMIP_UoM-CMIP-1-1-0_gr3-GMNHSH_0000-2014.csv
2. NOAA GML. Accessed 04-March-2022. https://gml.noaa.gov/ccgg/trends/gl_data.html
File: https://gml.noaa.gov/webdata/ccgg/trends/co2/co2_anmean_gl.txt
3. Global Carbon Budget: National_Carbon_Emissions_2021v0.4.xlsx Historical Budget, Global Fossil Emissions Visited 04 March 2022. Friedlingstein et al (2021),
4. World Data Service for Paleoclimatology, Boulder and NOAA Paleoclimatology Program, National Centers for Environmental Information (NCEI)
<https://www1.ncdc.noaa.gov/pub/data/paleo/icecore/antarctica/law/law2018d13c-co2.txt>,
<https://doi.org/10.25919/5bfe29ff807fb>
5. UNSCEAR: United Nations Scientific Committee on the Effects of Atomic Radiation 2000 Report To The General Assembly. Volume I: Sources. Annex C: Exposures To The Public From Man-Made Sources Of Radiation 207 Sources And Effects Of Ionizing Radiation. . Table 4. Annual Fission And Fusion Yields.
6. Calib: INTCAL20/SGCAL20. Stuiver, M. et al, 2022 CALIB 8.2 [WWW program] at <http://calib.org>, accessed 2022-3-4 Rev 8.1.0 intcal20.14c, shcal20.14c